The effect of pump wavelength, power and direction on gain and noise figure in double-pass/stage TDFAs

MURAT YUCEL*, AYTEN DINCER
Department of Electrical and Electronics Engineering, Gazi University, Ankara, Turkiye

The effects of pump laser wavelength, power, and direction on optical gain and noise figures in double pass/stage TDFA setups were investigated. For this purpose, four different setups with different pumping types are presented comparatively along the S-band. TDF lengths have been optimized and setups are aimed to be similar. By comparing the pumps with wavelengths of 800, 1050, 1400, and 1560 nm, which are widely used in the literature, the most efficient pump wavelength was determined. The effect of pump direction was investigated by using forward, backward, and bidirectional pumping methods. Then, the setups were compared and the pump power and pumping method were determined with the most efficient wavelength. Finally, the PCE values of all designs were examined and compared.

(Received January 30, 2023; accepted August 7, 2023)

Keywords: Thulium-doped fiber amplifier, Double-pass, Forward pumping, Backward pumping, Bidirectional pumping

1. Introduction

With the developing technologies, human needs and behaviors such as shopping learning, working, socializing and entertainment have turned to online implementations. This transformation has gained great momentum with the Covid-19 pandemic [1]. The use of high-bandwidth applications such as voice-over IP, video conferencing online gaming, social networks and high-definition (720p and above) video streaming has increased rapidly. While these new-generation technologies, the usage of which is increasing, require an increase in transmission speed and capacity, they also necessitate a change in the communication infrastructure. Fiber optic communication systems and optical amplifiers within these systems, which can provide more bandwidth with Wavelength Division Multiplexing (WDM), have a great role in meeting all these requirements [2-5]. The studies carried out so far have focused on Erbium-Doped Fiber Amplifiers (EDFAs) with high efficiency in the C and L bands [6-10]. Since C and L bands may be insufficient to meet the increasing demand, optical amplifiers research is carried out that can work efficiently in the S-band. Thulium Doped Fiber Amplifier (TDFA) and Fiber Raman Amplifier (FRA) are optical amplifiers with high efficiency in the S-band [11]. However, FRA has some limitations such as high pump power and the use of multiple pumps [12]. Therefore, TDFAs are seen as a better alternative in the S-band instead of FRA [13,14]. There are some TDFA studies done by changing basic parameters such as TDF length, pumping power and thulium ion density to achieve high gain and low noise figure values [15-20]. For the same purpose, there are some studies on different pumping methods to excite all Thulium ions [21-26]. In addition, research has been done on double pass configurations that increase the gain by adding a mirror or a circulator to the basic TDFA design [27-30]. There are studies conducted by separately pumping two different TDFs, some of which are called double-pass and some are called double-stage [30-32]. In some studies performed in the 1950 nm – 2000 nm band gap, the second of two different TDFs was fed by pumping back [33-35]. Besides parameters such as different configurations, pumping method, doped-fiber length and Thulium density, pumping wavelength also has a great importance on performance. When the literature is examined, considering the absorption and emission spectrum of Thulium; 690 nm [22], 800 nm [16, 17, 21, 24, 25], 1047 nm [23], 1050 nm [16, 22, 24, 25, 27, 28, 38], 1064 nm [13, 31], 1210 nm [32], 1400 nm [15-17, 21-23, 25], 1550 nm [23, 26], 1560 nm [35, 36, 38], 1567 nm [33, 34], 1570 nm [14, 37] pump wavelengths are found in studies. As can be seen, some pump wavelength values are close to each other, and first, in this study, the effects of pumps with 800 nm, 1050 nm, 1400 nm and 1560 nm wavelengths on the optical gain and noise values were investigated in double pass TDFA (DP-TDFA) and double-stage TDFA (DS-TDFA) setups where the input signal passes through TDF twice. Secondly, the pump power and pumping method were researched with the most efficient wavelength.

Finally, the output power of the input signal with 0 dBm power at 1469 nm wavelength was examined through all TDFA designs fed with varying pump powers. PCE values of all designs were defined using these output power values.

In this study, forward, forward-forward and forward-backward (bidirectional) pumped DS-TDFA designs in the literature were considered together, and the effects of the pumping direction on the gain and noise figure were examined and compared. In addition to the designs that have been tried so far, in this study, the pump power is divided into three, the first of TDF will be pumped

forward and the second is pumped forward and backward (bidirectional).

2. Theoretical analysis of TDFA

In this section, the theoretical equations referenced by the software used in the modeling are examined. In TDFAs, the gain depends on the ion density and population inversion of thulium ions at different energy levels [17]. Fig. 1 shows the energy levels of thulium ions in silica fiber [36]. The energy levels 0, 1, 2, 3, 5 are respectively named as $^3H_6$, $^3F_4$, $^3H_5$, $^3H_4$, $^1G_4$.

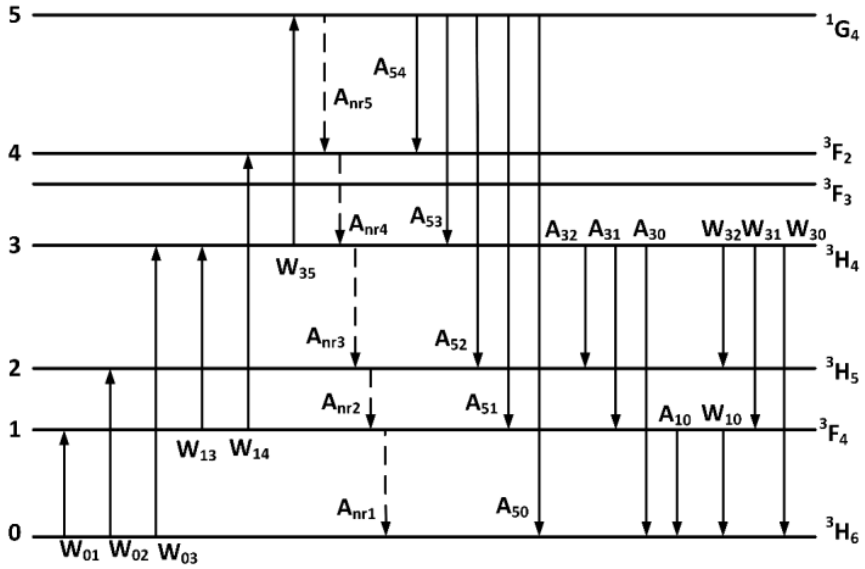

Fig. 1. Energy band diagram of thulium

The rate equation of the different energy levels of thulium was proposed by P. Peterka et al. as follows [36]:

$$\frac{dN_2}{dt}=N_0(W_{01}+W_{02})-N_1(W_{10}+W_{13}+W_{14}+A_1^{nr}+A_{10}^{r})+N_3(W_{31}+W_{32}+A_3^{nr}+A_{32}^{r}+A_{31}^{r}))+N_5(A_{51}^{r}+A_{52}^{r}) \quad (1)$$

$$\frac{dN_3}{dt}=N_0(W_{03})+N_1(W_{13}+W_{14})-N_5(A_5^{nr}+A_{52}^{r}+A_{53}^{r})-N_3(W_{35}+W_{32}+W_{31}+W_{30}+A_3^{nr}+\sum_{j=0}^{2}A_{3j}^{r}) \quad (2)$$

$$\frac{dN_5}{dt}=N_0(W_{05})+N_3W_{35}-N_5(W_{50}+A_5^{nr}+\sum_{j=0}^{4}A_{5j}^{r}) \quad (3)$$

$$N_t = N_0 + N_1 + N_3 + N_5 \quad (4)$$

where, the N_0, N_1, N_3, N_5 values represent the population density of $^3H_6$, $^3F_4$, $^3H_4$, $^1G_4$ levels, respectively. N_i and W_{ij} variables are functions of r, φ, z positions. Considering that the thulium ions are homogeneously excited in the fiber cross-section, the transition value expression describing the electromagnetic interaction of the ions can be written as W_{ij} in equation (5) [36].

$$W_{ij}(z)=\int_0^{\infty}\lambda\Gamma(\lambda)\sigma_{ij}(\lambda)\frac{\left(P_\lambda^+(z,\lambda)+P_\lambda^-(z,\lambda)\right)}{hc\pi b^2}\,d\lambda \quad (5)$$

where σij is the relevant cross-section, h is the Plank constant, c is the speed of light, P_λ^+ and P_λ^- are the spectral power density of the positive and negative diffuse emission of the fiber axis. $\Gamma(\lambda)$ is the overlap factor and is defined by equation (6) [36].

$$\Gamma(\lambda)=\frac{\int_0^{\infty}|E(r,\varphi,\lambda)|^2N(r)rdr}{N_t\int_0^{\infty}|E(r,\varphi,\lambda)|^2rdr} \quad (6)$$

For flexibility in choosing the number of pumps and wavelength, the same equation (7) is defined for the propagation of each forward segment of the wave [36].

$$\frac{dP^+(\lambda)}{dz}=\Gamma(\lambda)P^+(\lambda)\sum_{ij}^{\{10,30,31,50,32\}}\left(N_i\,\sigma_{ij}(\lambda)-N_j\,\sigma_{ji}(\lambda)\right)-\Gamma(\lambda)P^+(\lambda)(N_0\,\sigma_{02}(\lambda)+N_1\,\sigma_{14}(\lambda)+N_3\,\sigma_{35}(\lambda))+\Gamma(\lambda)\sum_{ij}^{\{10,30,31,50,32\}}2h\nu_{ij}\Delta\nu N_i\,\sigma_{ij}(\lambda)-\alpha(\lambda)\,P^+(\lambda) \quad (7)$$

At certain boundary states of z=0 and z=L, the problem is reduced to a steady state when the time derivatives $\frac{dN_1}{dt}$, $\frac{dN_2}{dt}$, $\frac{dN_3}{dt}$ are set to zero. L is the length of the fiber amplifier. To obtain the gain characteristic of TDFA, the equation is completed over space and frequency.

3. TDFA designs

DP-TDFA and all DS-TDFA designs are shown in Fig. 2, respectively. As can be seen in Fig. 2(a), a circulator and a mirror are added to the basic TDFA setup in the DP-TDFA design, and the reflected signal is passed over the TDF again, resulting in a second amplification of the signal. In the design named Double-Stage Forward-Forward Pumped TDFA (DSFFP-TDFA) in Fig. 2(b), the pump power is divided equally by using a power splitter and fed two different TDFs forward. In the design named Double-Stage Forward-Backward Pumped TDFA (DSFBP-TDFA) in Fig. 2(c), the pump power is divided into two as DSFFP-TDFA, but differently, the second TDF is fed by backward pumping. In this way, the effect of backward pumping on the gain and noise figure values has been investigated. There is an isolator between TDF 1 and TDF2 to separate stages from each other. Finally, in the design shown in Fig. 2(d), DSFFP-TDFA and DSFBP-TDFA designs are combined and the pump power is divided into three. This design is named Double-Stage Forward-Bidirectional Pumped TDFA (DSFBiP-TDFA). In Fig. 2a, light passes through a TDF twice, and in other figures, it passes through separate TDFs once and passes twice in total.

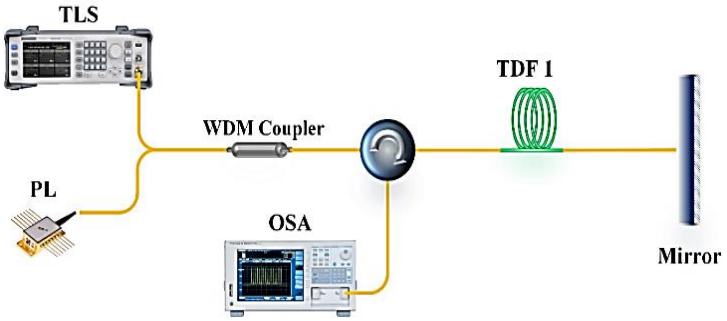

(a) DP-TDFA

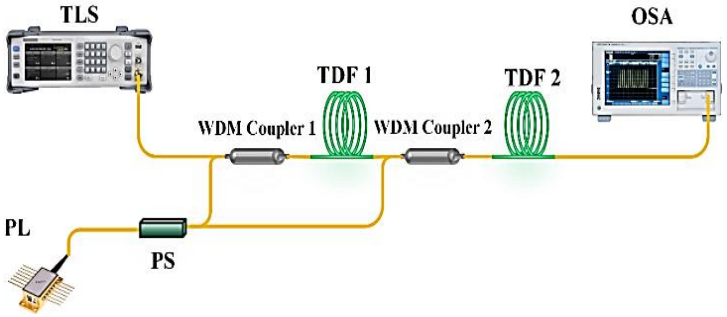

(b) DSFFP-TDFA

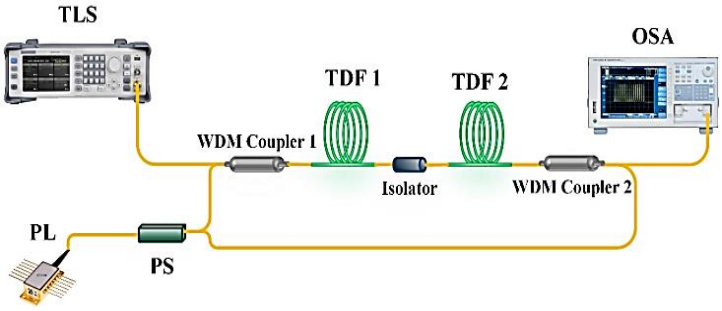

(c) DSFBP-TDFA

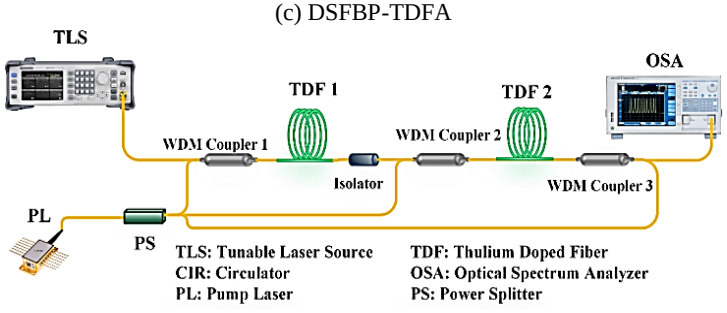

(d) DSFBiP-TDFA

Fig. 2. DP-TDFA and DS-TDFA designs (color online)

In the first part, each design, according to the results of the previous study [30], has -20 dBm input power, 1469 input signal and 1000 mW pump power; it has been simulated separately by feeding with pumps at wavelengths of 800 nm, 1050 nm, 1400 nm and 1450 nm. Gain and noise figure graphs have been created using the obtained values, and the most efficient pump wavelength has been determined.

In the second part, using the pump wavelength determined in the first part, each design is separately simulated by increasing 200 mW each time at pump powers between 200 mW and 2000 mW. The data to be used in the study to be conducted in each section are listed in Table 1. As seen in it, 5+5 m TDF length has been used in all designs except DP TDFA. To provide the same conditions, in DP TDFA, 5 m was chosen because the signal passes through the same TDF twice.

Table 1. Pump wavelengths, pump powers, and pumping directions of all designs used in the first simulations

Designs	Pump Wavelength (nm)	Pump Power (mW)	Pump Direction	TDF Length (m)
DP-TDFA	800, 1050, 1400, 1560	1000	Forward	5
DSFFP-TDFA	800, 1050, 1400, 1560	500+500	Forward + Forward	5+5
DSFBP-TDFA	800, 1050, 1400, 1560	500+500	Forward + Backward	5+5
DSFBiP-TDFA	800, 1050, 1400, 1560	333+333 +333	Forward + Bidirectional	5+5

All TDFAs were simulated using the Optiwave 19.0 software program. Optiwave is a professional commercial software and is supported by many proven articles in the literature [39-42]. The parameters used in all simulations are listed in Table 2 and Tm emission cross-section spectra are shown in Fig. 3.

Table 2. Parameters used in the simulation

Parameter	Value	Unit
Numerical Departure	1	
Core Radius	1.3	μm
Doping Radius	0.8	μm
Thulium Ion Concentration	20e + 024	m^{-3}
Non-radiant ion lifetime 1	430×10^{-6}	s
Non-radiant ion lifetime 2	45×10^{-6}	s
Non-radiant ion lifetime 3	784×10^{-6}	s
Ar10	285.7	*(1/s)*
Ar30	1353.85	*(1/s)*
Ar31	138.46	*(1/s)*
Ar32	46.153	*(1/s)*
Ar50	581.4	*(1/s)*

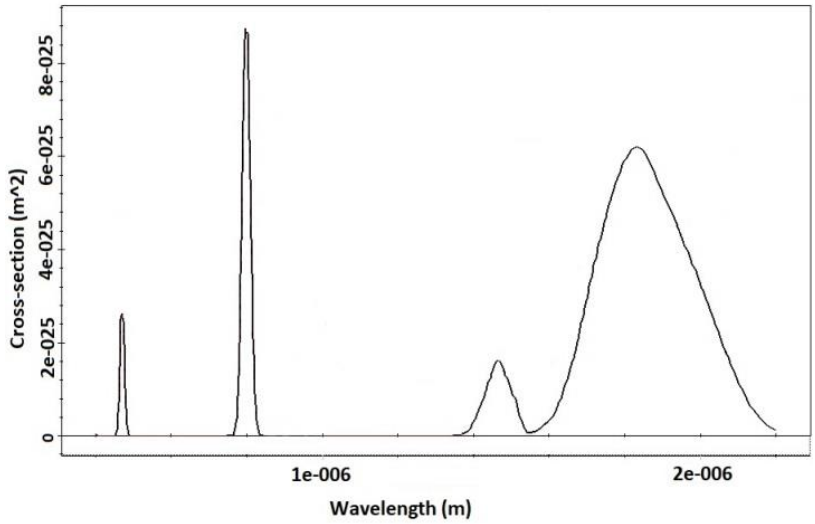

Fig. 3. Tm emission cross-section spectra used in the simulation

4. Simulation results

The gain and the noise figure values have been obtained by simulating all TDFA designs separately. These values are shown in two separate graphs as gain and noise figures for easy comparison.

Firstly, 1000 mW power pumps at different wavelengths have been applied to the input signals of -20 dBm power at 1469 nm wavelength. Fig. 4 shows the gain and noise figure graphs of DP/DS-TDFA designs fed by pumps at wavelengths of 800 nm, 1050 nm, 1400 nm and 1560 nm.

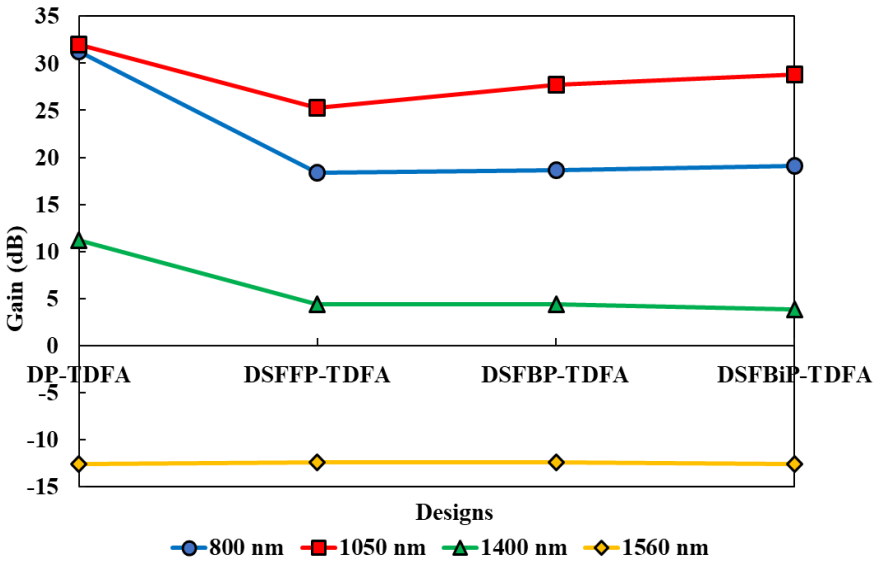

(a) Gain

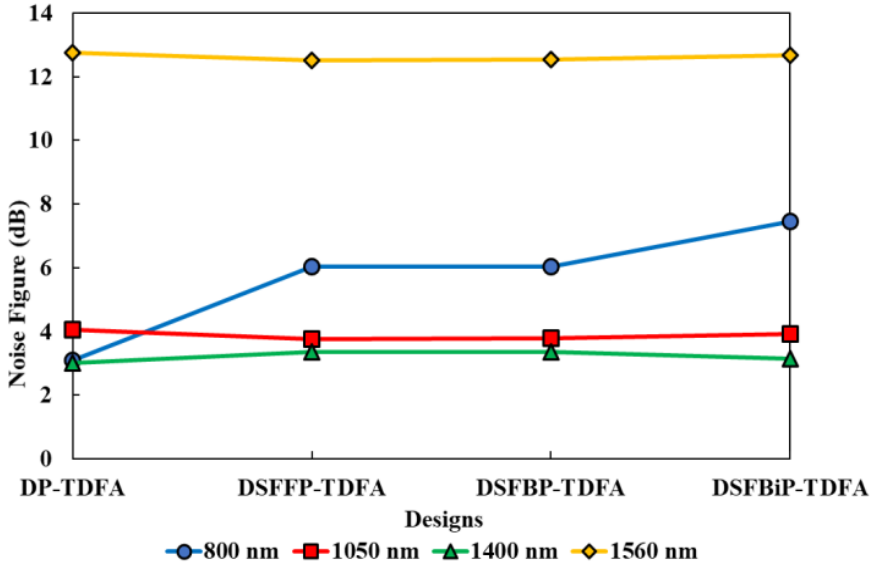

(b) Noise figure

Fig. 4. (a) Gain and (b) Noise figure graphs of all designs fed at different pump wavelengths (color online)

When the graph in Fig. 4(a) is examined, it is seen that the highest gain values are obtained at the pump wavelength of 1050 nm. In Fig. 4(b), it can be seen that designs pumped at wavelengths of 1050 nm and 1400 nm generate lower noise figures when compared to the other designs. According to these results, the most efficient pump wavelength for all DP/DS-TDFA designs in the S-band is determined as 1050 nm.

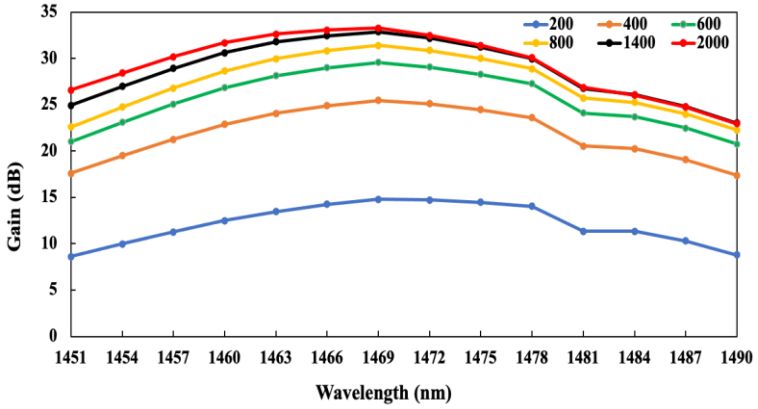

(a) DP-TDFA

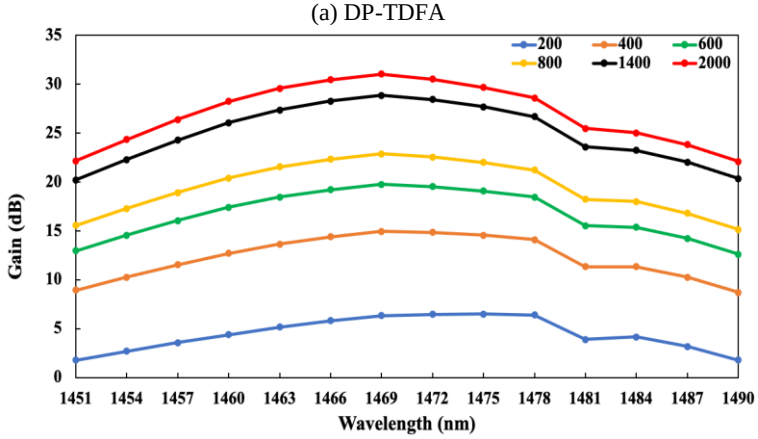

(b) DSFFP-TDFA

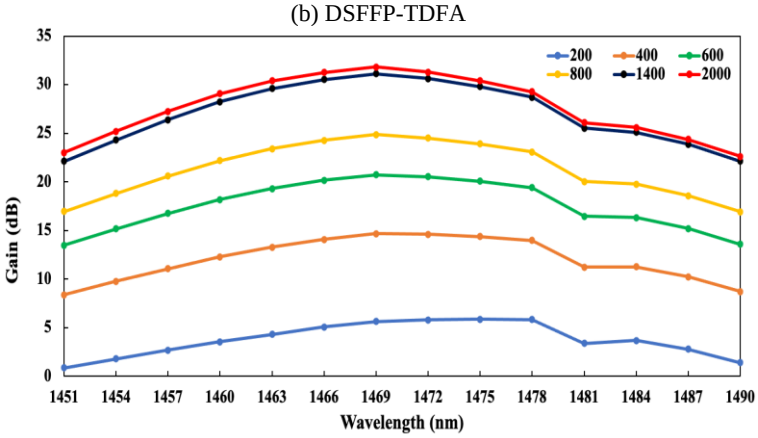

(c) DSFBP-TDFA

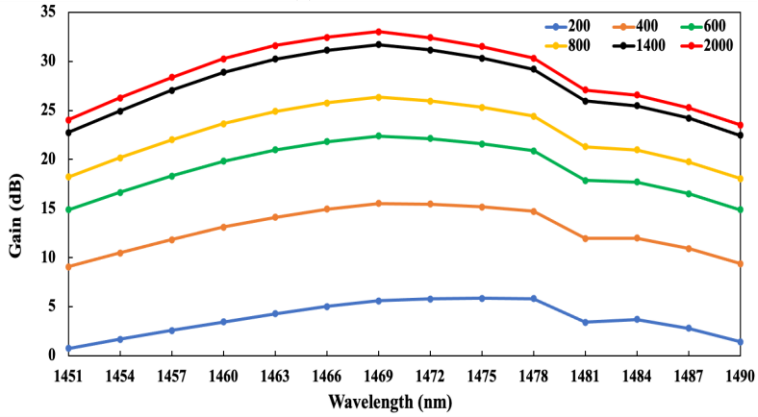

(d) DSFBiP-TDFA

Fig. 5. The gain spectra of all designs at different pump powers (mW) (color online)

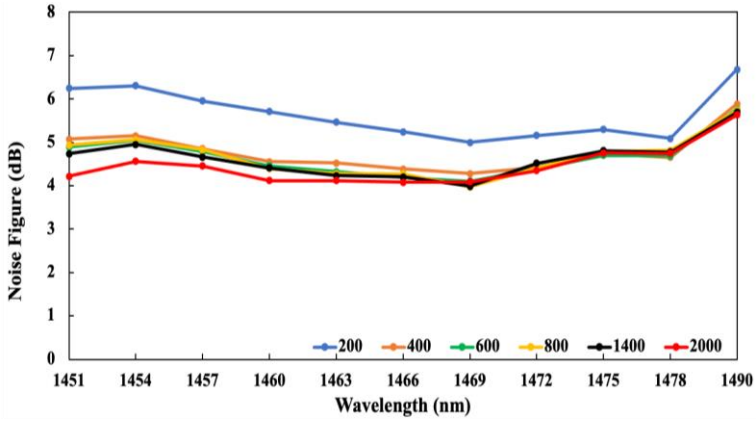

(a) DP-TDFA

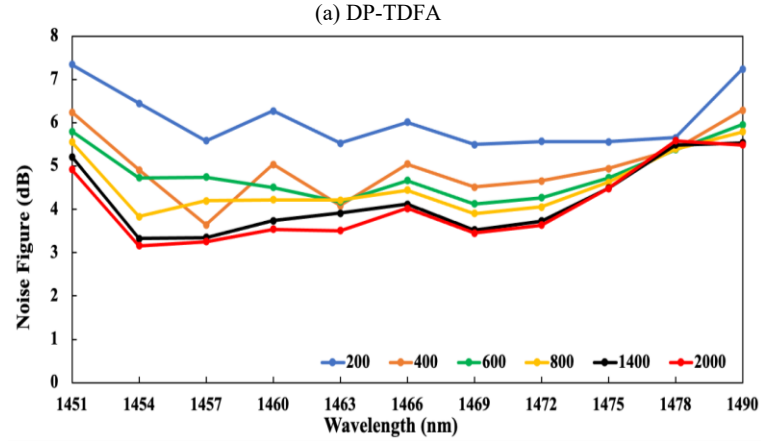

(b) DSFFP-TDFA

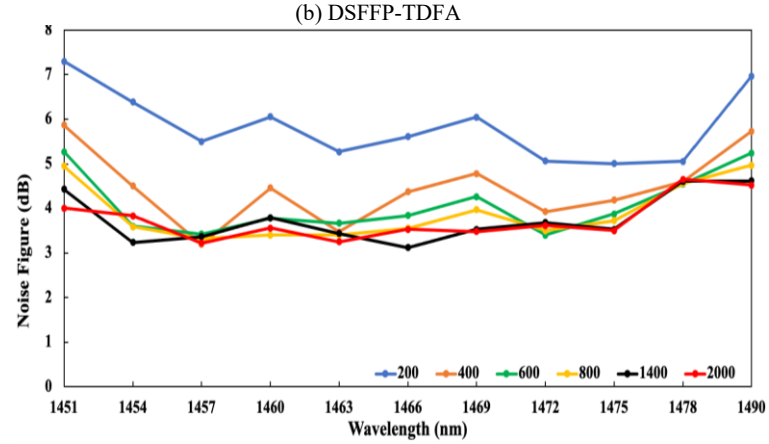

(c) DSFBP-TDFA

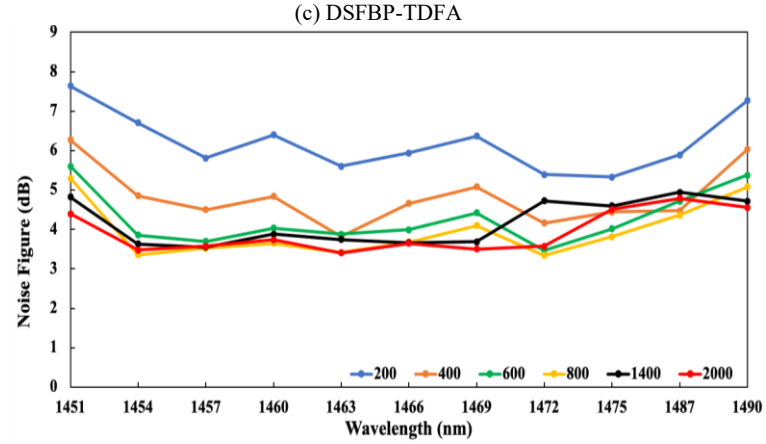

(d) DSFBiP-TDFA

Fig. 6. Noise figure spectra of all designs at different pump powers (mW) (color online)

Secondly, the pump power and pumping direction studies have been carried out using a pump with a wavelength of 1050 nm. Each design is separately simulated by increasing 200 mW each time at pump powers between 200 mW and 2000 mW. However, to improve the readability of the graphs, some of the close results are not indicated in the graph. Input signals' wavelengths are applied between the range of 1451-1490 nm. When Fig. 5 is examined, it is seen that the DP-TDFA approaches saturation after 800 mW of pump power, and the effect of pump power increase on the system gain is low. In this design, the gain values at low pump powers are higher compared to other designs. Because, unlike other designs, it uses all the power of the pump without dividing. For this design, 800 mW or 1000 mW of pump power can be considered as the optimum value.

Since the pump power is shared in other designs, it is seen that the gain increase continues, albeit slightly, up to 2000 mW pump power. It is seen that the gain in the DSFBP-TDFA with backward pumping is higher than the DSFFP-TDFA with forward pumping. When choosing the second pumping method, using backward pumping instead of forward pumping increased the gain value. This is because the signal is strong near the pump input end, holding the excitation density down in that region so that the pump light is efficiently absorbed by the ions before parasitic losses can get it. Additionally, bidirectional pumping maybe even more efficient. The gain value is further increased in the DSFBiP-TDFA, which is a combination of designs (b) and (c). Considering all the designs, the gain values of setups (a) and (d) are close to each other and have the highest values. It is seen that the gain of setup 4 can continue to increase when the pump power is increased.

In Fig. 6, noise figure spectra of all designs at different pump powers are given. According to the graphs, the lowest noise figure levels vary according to the signal wavelength and pump power. Noise figure values are high in all designs at 200 mW and 400 mW pump powers. The increase in pump power causes a general decrease in noise figure levels. The lowest noise figure is observed in the band range of 1454-1475 nm. The highest noise figure values have occurred in the DP-TDFA design. This increase is attributed to the higher counter-propagating ASE at the input part of the amplifier. This reduces the population inversion at the input part of TDF and afterward increases the noise figure [29]. The noise values of DSFBP-TDFA and DSFBiP-TDFA designs are close to each other and the lowest values are in these two designs.

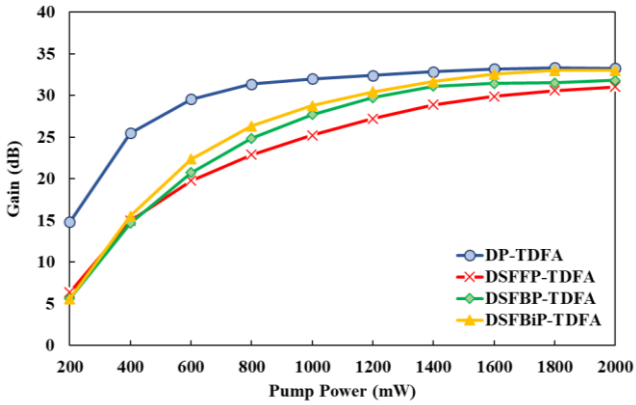

(a) Pump power-Gain

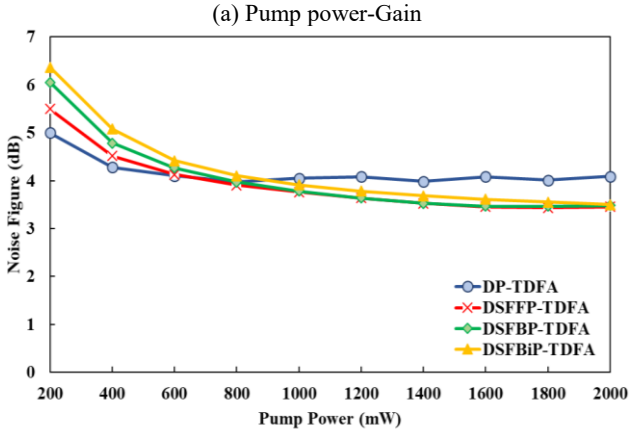

(b) Pump power-Noise figure

Fig. 7. Pump power versus gain and pump power versus noise figure spectra of all designs at 1469 nm (color online)

For easier comparison, the gain values at 1469 nm wavelength in the pump power variation study are combined in the graph in Fig. 7(a). Similarly, Fig. 7(b) has been created using noise figure values at 1469 nm wavelength. In DP-TDFA, the amplifier saturates at low pump powers in response to low fiber length. It is seen that the gain continues to increase as the pump power increases in the designs with separate pumping. The gain values of DSFFP-TDFA, which is pumped forward, and DSFBP-TDFA, which is pumped backward, are close until the pump power is 600 mW. At power values above 600 mW, the gain values are higher up to 1600 mW, showing the effect of backward pumping. However, considering the graph curve, after 1400 mW of pump power, the backward-pumped DSFBP-TDFA seems to have reached saturation, while the forward-pumping DSFFP-TDFA continues to increase the gain. When the graph is examined, the optimum pump powers can be said that 800 mW for DP-TDFA, 2000 mW for DSFFP-TDFA, 1400 mW for DSFBP-TDFA and 1600 mW for DSFBiP-TDFA.

According to the pump power-noise figure plot in Fig. 7(b), 400 mW is the pump power threshold for DP-TDFA. While the noise figure decreases up to this value, it changes very little since the amplifier reaches saturation after that. In the other designs, the noise figure values

decrease with the increase of the pump power, as the amplifier gain increases and approaches saturation.

Finally, the output power variation of the input signal at 0 dBm power at 1469 nm wavelength has been investigated. A 1050 nm wavelength, varying power pump has been used. Power Conversion Efficiency (PCE) has been calculated using these output power values.

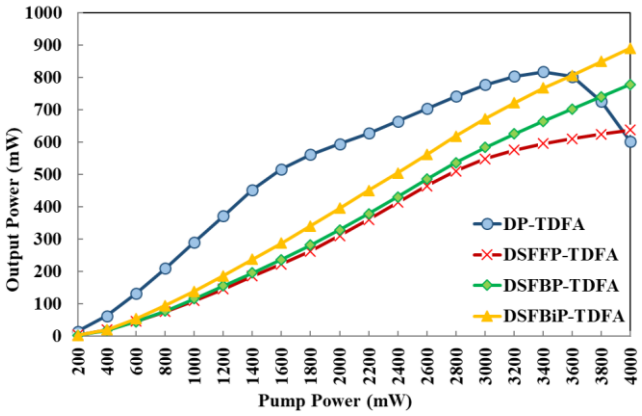

(a) Output power-Pump power

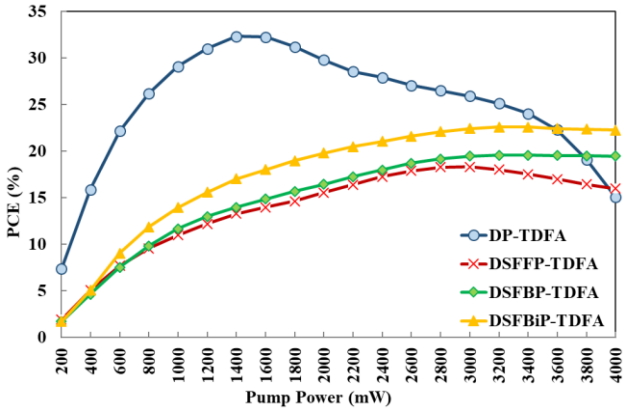

(b) PCE-Pump power

Fig. 8. Output power versus pump power end PCE versus pump power spectra of all designs (color online)

The spectra of output power and PCE in the pump power variation of all designs are combined in the graph in Fig. 8 using the values at 1469 nm wavelength. As seen in Fig. 8(a), while the output power is high in DP-TDFA design at low pump powers, the slope of the rise decreased after 1800 mW. After 3400 mW pump power, it started to decline. In other designs, the output power rise slope is close to each other and the highest values are in the DSFBiP-TDFA design. In DSFBP-TDFA and DSFBiP-TDFA designs with backward pumping the increase in output power continues with the increase in pump power.

PCE values of all designs are shown in Fig. 8(b). The PCE of the DP-TDFA design is high and reaches the maximum value of 32.32% at 1400 mW pump power. The PCE decrease for the pump powers after this value. PCE of backward pumped DSFBP-TDFA and DSFBiP-TDFA designs increase with increasing pump power. The highest PCE is 19.56% for DSFBP-TDFA and 22.56% for DSFBiP-TDFA at 3400 mW pump power.

5. Conclusion

In this study, DP, DSFFP, DSFBP, and DSFBiP-TDFA designs have been created. It is the first time that DSFBiP-TDFA is used in S-band in the literature. All DP-TDFA designs have been fed by pumps at wavelengths of 800 nm, 1050 nm, 1400 nm and 1560 nm to find the efficient pump wavelength. According to the results, the most efficient pump wavelength for all DP- TDFA designs in the S-band has been determined as 1050 nm.

Then, the pump power and pumping direction have been researched using a pump at 1050 nm wavelength. When the figures are examined, the optimum pump powers can be said that 800 mW for DP-TDFA, 2000 mW for DSFFP-TDFA, 1400 mW for DSFBP-TDFA and 1600 mW for DSFBiP-TDFA. It is also seen that the gain in the DSFBP-TDFA with backward pumping is higher than the DSFFP-TDFA with forward pumping. When choosing the second pumping method, using backward pumping instead of forward pumping increased the gain. Since the signal is strong near the pump input end, it keeps the excitation intensity in that area low so that the pump light is efficiently absorbed by the ions before parasitic losses pick up on it.

Finally, the output power of the input signal with 0 dBm power at 1469 nm wavelength has been examined through all TDFA designs fed with varying pump powers. PCE values of all designs are examined using these output power values. The PCE values of the DP-TDFA design are high and reach the maximum value of 32.32% at 1400 mW pump power. The highest PCE values are 19.56% for DSFBP-TDFA and 22.56% for DSFBiP-TDFA at 3400 mW pump power. While DP-TDFA is efficient for designs using pump power below 3400 mW, using DSFBiP-TDFA in designs pumping above this power will provide more efficient results.

From the obtained results, while DP TDFA will be the best practical design at low pump powers, DS-TDFAs are more efficient at high pump powers. As for DS-TDFAs, the backward pumping design is more advantageous than the forward pumping design. On the other hand, bidirectional design in addition to forward pumping gave more gain, especially at high pump powers.

References

[1] D. Vargo, L. Zhu, B. Benwell, Z. Yan, Hum. Behav. Emerg. Tech. **3**, 13 (2021).
[2] Y. Sun, A. K. Srivastava, J. Zhou, J. W. Sulhoff, Bell. Labs. Tech. J. **4**(1), 187 (1999).
[3] S. Singh, A. Singh, R. S. Kaler, Optik **124**(2), 95 (2013).
[4] X. Ding, G. Wu, F. Zuo, J. Chen, Optoelectronics Letters **15**(6), 401 (2019).

[5] D. Malik, G. Kaushik, A. Wason, J. Opt. **47**(3), 396 (2018).
[6] M. Yücel, H. H. Göktas, G. Akkaya, 2012 20th Signal Processing and Communication Applications, 1 (2012).
[7] M. Yucel, Z. Aslan, Microw. Opt. Technol. Lett. **55**, 2525 (2013).
[8] J. A. Bebawi, I. Kandas, M. A. El-Osairy, M. H. Aly, Appl. Sci. **8**(9), 1640 (2018).
[9] N. M. Anwar, Z. El-Sahn, E. A. El-Badawy, M. H. Aly, Opt. Quant. Electron. **52**, 109 (2020).
[10] O. Akcesme, M. Yucel, M. Burunkaya, Optik **239**, 166850 (2021).
[11] J. Kani, M. Jinno, Electron. Let. **35**(2), 1004 (1999).
[12] S. Zhu, S. Pidishety, Y. Feng, S. Hong, J. Demas, R. Sidharthan, S. Yoo, S. Ramachansran, B. Srinivasan, J. Nilsson, Opt. Express **26**(18), 23295 (2018).
[13] A. H. M. Husein, F. I. El-Nahal, Optik **124**(19), 4052(2012).
[14] Z. Li, A. M. Heidt, J. M. O. Daniel, Y. Jung, S. U. Alam, D.J. Richardson, Opt. Express **21**(8), 9289 (2013).
[15] S. Aozasa, H. Masuda, M. Shimizu, J. Lightwave Technol. **24**(10), 3842 (2006).
[16] F. I. El-Nahal, A. Hakeim, N. Husein, Open Journal of Applied Sciences **2**(4), 5 (2012).
[17] R. Singh, M. L. Singh, 2016 International Conference on Recent Advances and Innovations in Engineering, 1 (2016).
[18] I. Kaur, N. Gupta, International Journal of Computing and Digital Systems **3**(3), 227 (2014).
[19] K. P. W. Dissanayakel, S. D. Emami, H. A. Abdul-Rashidi, S. M. Aljamimi, Z. Yusoff, M. I. Zulkifli, S. Z. Muhamad-Yassin, K. A. Mat-Sharif, N. Tamchek, 2013 IEEE 4th International Conference on Photonics (ICP), 288 (2013).
[20] M. Yücel, A. Dincer, Düzce Üniversitesi Bilim ve Teknoloji Dergisi **8**(3), 2062 (2020).
[21] R. Singh, M. L. Singh, B. Kaur, Optik **123**(20), 1815 (2012).
[22] S. H. Yam, Y. Akasaka, Y. Kubota, H. Inoue, K. Parameswaran, IEEE Photonics Technology Letters **17**(5), 1001 (2005).
[23] F. Roy, D. Bayart, A. Sauze, P. Baniel, IEEE Photonics Technology Letters **13**(8), 788 (2001).
[24] A. S. L. Gomes, M. T. Carvalho, M. L. Sundheimer, C. J. A. Bastos-Filho, J. F. Martins-Filho, M. B. Costa e Silva, J. P. von der Weid, W. Margulis, IEEE Photonics Technology Letters **15**(2), 200 (2003).
[25] R. Singh, M. L. Singh, Optik **140**, 565 (2017).
[26] M. S. K. Jamalus, N. M. Yusoff, A. H. Sulaiman, Indonesian J. of Elect. Eng. and Com. Science **15**(3), 1203 (2019).
[27] S. D. Emami, S. W. Harun, H. A. Abdul-Rashid, S. A. Daud, H. Ahmad, Progress in Electromagnetics Research B. **14**, 431 (2009).
[28] C. J. A. Bastos-Filho, J. F. Martins-Filho, The 2003 SBMO/IEEE MTT-S International Microwave and Optoelectronics Conference **1**, 125 (2003).
[29] S. D. Emami, S. W. Harun, H. A. Abdul-Rashid, S. A. Daud, H. Ahmad, F. Abd-Rahman, Z. A. Ghani, Optik **121**(4), 1257 (2010).
[30] M. Yucel, A. Dincer, Micro. Opt. Tech. Lett. **64**(10), 1863 (2022).
[31] D. Mohammed, A. Hammadi, Journal of Optical Communications https://doi.org/10.1515/joc-2020-0313 (2021).
[32] J. Mirza, A. Atieh, M. I. Menhas, S. Ghafoor, M. Magam, L. Jamal, S. I. M. Sheikh, K. K. Qureshi, Ain Shams Engineering Journal, to be published.
[33] R. E. Tench, A. Amavigan, K. Chen, J. M. Delavaux, T. Robin, B. Cadier, A. Laurent, IEEE Photonics Technology Letters **32**(15), 956 (2020).
[34] R. E. Tench, C. Romano, J. M. P. Delavaux, Applied Optics **57**(21), 5948 (2018).
[35] S. D. Emami, S. W. Harun, F. Abd-Rahman, H. A. Abdul-Rashid, H. Ahmad, Laser Phys. **18**, 977 (2008).
[36] P. Peterka, B. Faure, W. Blanc, M. Karasek, B. Dussardier, Optical and Quantum Electronics **36**, 201 (2004).
[37] M. Khamis, K. Ennser, Journal of Lightwave Technology **34**(24), 5675 (2016).
[38] T. Kasamatsu, Y. Yano, H. Sekita, Optics Letters **24**(23), 1684 (1999).
[39] R. Miglani, G. Singh, G. Singh, D. P. Agrwal, J. Opt. **49**, 323 (2020).
[40] M. H. Ali, F. Abdullah, T. F. Al-Mashhadani, Opt. Quant. Electron. **52**, 386 (2020).
[41] A. K. Abass, M. H. Ali, M. A. Saleh, F. F. Rashid, Journal of Optics (published online 31 December 2022, https://doi.org/10.1007/s12596-022-01074-w).
[42] A. Kaur, M. S. Bhamrah, A. Atieh, Optical Fiber Technology **52**, 101971 (2019).

*Corresponding author: muyucel@gazi.edu.tr